UWB RSS-Based Localization for Capsule Endoscopy Using a Multilayer Phantom and *In Vivo* Measurements

Martina Barbi, Concepcion Garcia-Pardo, Andrea Nevárez, Vicente Pons Beltrán, and Narcís Cardona, *Member, IEEE*

***Abstract*— In recent years, the localization for capsule endoscopy applications using ultrawideband (UWB) technology has become an attractive field of investigation due to its potential benefits for patients. The literature concerning performance analysis of radio frequency-based localization techniques for in-body applications at UWB frequencies is very limited. Available studies mainly rely on finite-difference time-domain simulations, using digital human models and on experimental measurements by means of homogeneous phantoms. Nevertheless, no realistic analysis based on multilayer phantom measurements or through *in vivo* experiment has been reported yet. This paper investigates the performance of the received signal strength-based approach for 2-D and 3-D localizations in the UWB frequency band. For 2-D localization, experimental laboratory measurements using a two-layer phantom-based setup have been conducted. For 3-D localization, data from a recently conducted *in vivo* experiment have been used. Localization accuracy using path loss models, under ideal and non-ideal channel estimation assumptions, is compared. Results show that, under nonideal channel assumption, the relative localization error slightly increases for the 2-D case but not for the *in vivo* 3-D case. Impact of receivers selection on the localization accuracy has also been investigated for both 2-D and 3-D cases.**

***Index Terms*— Heterogeneous phantom, in-body localization, *in vivo* measurements, ultrawideband (UWB), wireless capsule endoscopy (WCE).**

I. Introduction

WIRELESS capsule endoscopy (WCE) is a revolutionary invention introduced in the medical sector several years ago. A tiny capsule, equipped with a camera, is swallowed by the patient. As it travels along the gastrointestinal (GI) tract, it takes thousands of pictures (up to 6 per seconds) and sends them to an external recorder located on a belt around the patient's waist. When the recorder is returned, the physician is able to visualize a video of the whole patient's small bowel and detect potential abnormalities by visual inspection. However, the images provided by current capsule endoscope are not very high quality [1]. Moreover, a precise localization of anomalies is highly important for their subsequent treatment. In fact, the position estimation of the pill is currently very inaccurate by using proprietary software applications provided to hospitals [2], [3] so the doctor cannot precisely locate detected diseases. In addition, not only the precise location but also an accurate tracking of the capsule is of fundamental importance for the future of this technology [4].

In the literature, many different approaches are available to locate the capsule endoscope. Several techniques use the radio frequency (RF) signals [5], [6], others magnetic fields [7], [8], and others imaging processing techniques [9]–[11].

RF-based localization inside the human body is an evolution of RF technology applied to indoor localization. Therefore, in the literature, the same techniques used for indoor localization are being investigated and adapted for capsule endoscope localization. However, in this case, the presence of the body tissues, instead of air, is even more problematic for the localization procedure, specifically in the ultrawideband (UWB) frequency band. In fact, the human body consists of different types of tissue each having its own electromagnetic properties. Particularly, permittivity and conductivity vary over different tissues and present values much higher than those of the air. Moreover, these electromagnetic properties are frequency-dependent. Consequently, the RF signal at UWB frequencies suffers from large frequency-dependent attenuation and severe multipath conditions, which makes ranging distance estimation very challenging. Despite these issues, the use of the RF signal, that the WCE uses for images transmission, also for localization purposes constitutes an optimal solution to keep the hardware of the capsule simple. Through this approach, first, a ranging estimation is performed. Second, the coordinates of the in-body source are calculated through trilateration methods. Ranging estimation is commonly accomplished by using distance-dependent parameters such as received signal strength (RSS) [12], time of arrival (ToA) [12], [13], time difference of arrival (TDoA) [13], or phase difference of arrival (PDoA) [14], [15]. In particular, RSS-based localization is commonly implemented due to its simplicity [12], [16]. Using this approach, the ranging estimation is performed,

Manuscript received March 1, 2018; revised February 14, 2019; accepted April 8, 2019. Date of publication May 20, 2019; date of current version August 12, 2019. This work was supported in part by the European Union's H2020 through the MSCA:ITN Program "Wireless in-Body Environment Communication—WiBEC" under Grant 675353, in part by the Programa de Ayudas de Investigación y Desarrollo, Universitat Politècnica de València under Grant PAID-01-16, and in part by the Ministerio de Economía y Competitividad, Spain, through the European FEDER Funds under Grant TEC2014-60258-C2-1-R. *(Corresponding author: Martina Barbi.)*

M. Barbi, C. Garcia-Pardo, and N. Cardona are with iTEAM, Universitat Politècnica de València, 46022 Valencia, Spain (e-mail: marbar6@iteam.upv.es; cgpardo@iteam.upv.es; ncardona@iteam.upv.es).

A. Nevárez and V. Pons Beltrán are with the Hospital Universitari i Politècnic La Fe, Digestive Diseases Area, 46126 Valencia, Spain (e-mail: nevarezja78@gmail.com; pons_vicbel@gva.es).

Color versions of one or more of the figures in this paper are available online at http://ieeexplore.ieee.org.

Digital Object Identifier 10.1109/TAP.2019.2916629

estimating the attenuation suffered by the received signal and relating this with a previously established model of the attenuation as a function of the distance from the source [path loss (PL) model]. Thus, the localization performance highly relies on the accuracy of the model [4].

Current capsule endoscopes operate in the Medical Implant Communication Service (MICS) frequency band (402–405 MHz). Although this band offers good penetration of the signal for in-body applications, the data rate (up to 500 Kb/s) is too low to support high-quality images [1]. In order to achieve this goal, in recent years, UWB technology has been under investigation for future capsule endoscopes due to its many advantages [17]. Particularly, the lowest part of the UWB spectrum (3.1–5.1 GHz) is being considered in the literature due to the unaffordable signal attenuation above this frequency range [18].

Currently, the performance analysis of RF-based localization techniques in the MICS frequency band is widely available [19]. On the contrary, studies conducted in the UWB frequency band are very limited. For RSS-based ranging, the main issue is the lack of standardized PL models for in-body to on-body communications at UWB frequencies.

Results through RF-based signals and compressive sensing are obtained in [16] using the computer simulation technology (CST) simulator with a finite integration technique (FIT) solver in 1–3 GHz and 3–5 GHz frequency bands. The best performance showed a mean localization error of 40 mm. The RSS-based approach is investigated in [20] by using an FIT simulator in the 1–6 GHz frequency band, showing a localization accuracy in the centimeters range. Kanaan and Suveren [21] address the crucial problem of ranging UWB signals inside the human body using XFDTD software platform in 3.4–4.8 GHz frequency range. Measurement campaign at 2–2.4 GHz using a homogeneous phantom model to investigate the influence of body tissue on the accuracy of ToA-based ranging technique is presented in [22]. Besides possible inaccuracy of the UWB phantom model used, homogeneous phantoms only emulate one human tissue; therefore, they cannot model with sufficient accuracy of the complex human body scenario.

Performing UWB heterogeneous phantoms-based measurements is not as simple as for the homogeneous phantom case because of the complexity to accurately mimic the electromagnetic properties of different human tissues in the whole UWB frequency band. Recently, researchers at the Universitat Politècnica de València (UPV) [23]–[25] have accomplished with this necessity. Furthermore, a customized measurement setup, presented in Section III-A, has been proposed in order to improve the measurement accuracy for in-body scenarios [26]. Regarding *in vivo* measurements, experiments in living animals are not easy to conduct as they are subject to ethical restrictions and extremely costly as dedicated facilities and a specialized medical team are required. Despite these difficulties, *in vivo* measurements, as previously pointed out, are the most realistic approach for in-body radio channel characterization and thus for the testing of RF-based localization techniques.

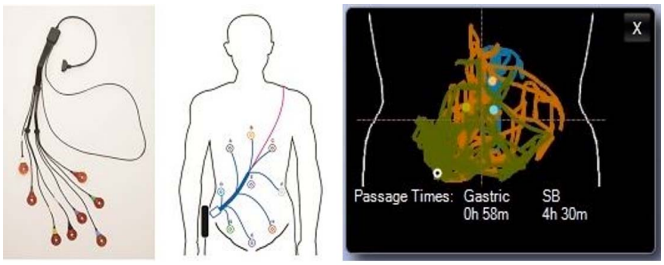

Fig. 1. (a) Sensor array and (b) movement pattern drawn by the software provided by the Medtronic technique [3].

To the best of the authors' knowledge, no implementation of RF-based localization techniques at UWB frequencies, using either an experimental heterogeneous phantom or through *in vivo* experiments, has been reported yet. In particular, *in vivo* measurements are of high relevance in order to test developed localization algorithms in a scenario that is the closest to reality, compared to laboratory measurements (controlled environment) and simulations (ideal environment).

In this paper, the performance of the RSS-based localization technique for UWB in-body to on-body (IB2OB) communications is investigated. To this aim, laboratory measurements using a customized multilayer phantom-based testbed as well as *in vivo* experiment have been conducted. Localization results obtained for both the measurement campaigns are then compared, in order to analyze the performance in the case of an emulated WCE scenario (laboratory) and in the case of a most realistic one (*in vivo*). The 2-D localization is performed based on the experimental laboratory measurements, while 3-D positioning is performed through the *in vivo* data.

The remainder of this paper is organized as follows. Section II briefly describes the real WCE scenario and the one emulated through experimental measurements. Section III presents the experimental measurements campaign conducted in the laboratory as well as the *in vivo* experiment. Section IV describes the RSS-based ranging technique, assuming ideal and nonideal channel estimations, as well as the localization algorithms used to evaluate the results for the 2-D and 3-D cases. Results are presented and discussed in Sections V and VI, respectively, along with the future research plans. Finally, Section VII concludes this paper.

II. Application Scenario

In the present WCE procedures, in order to locate the capsule endoscope, a sensors array [3], as shown in Fig. 1(a), is placed on the patient's body to receive transmission data from the pill while it is moving along the GI tract.

The information collected by the sensors is then processed offline by the software provided to the hospitals in order to visually draw the movement pattern [Fig. 1(b)] of the capsule traveling along the GI tract, depending on the landmark chosen by the physician. The mean localization error provided by, for example, the widely used Medtronic software, is roughly 3.8 cm [27].

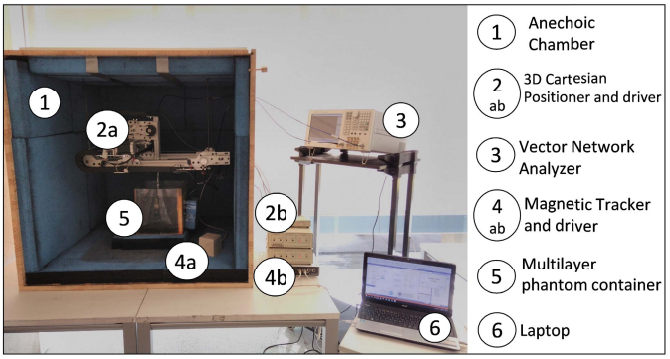

Fig. 2. Measurement testbed [26].

With the aim of reproducing the real in-body to on-body scenario [Fig. 1(a)] for localization purposes, laboratory and *in vivo* measurements, described in Sections III-A and III-B, were performed using a small UWB patch antenna, as the in-body source, designed to operate inside the human body [28] since there are currently no capsule endoscopes operating at these frequencies. A receiving UWB patch antenna, specifically designed to operate on the surface of the human body [29], was placed in different on-body locations in order to emulate the sensor array [Fig. 1(a)] currently used in the capsule endoscopy procedure. The collected data were then processed offline in order to locate the in-body source in 2-D and 3-D, as explained in Section IV.

III. Measurement Setup and Methodology

A. Phantom Measurements

Experimental measurements, using a multilayer phantom-based setup, were conducted in the 3.1–8.5 GHz UWB frequency band. A brief description of the testbed (Fig. 2) is given here, and further details can be found in [26].

All the equipment involved in the setup is software driven by a laptop (Fig. 2, element 6). The 3-D Cartesian positioner (Fig. 2, element 2a) accurately moves the in-body antenna along the *xyz*-axis inside the two-layer phantom container (Fig. 2, element 5).

The WCE scenario involves different human tissues, mainly colon, muscle, and fat. As colon and muscle have a similar permittivity, the phantom container was designed, specifically for muscle and fat layers. Muscle phantom is widely used in the literature for in-body to on-body communication studies. Moreover, the one created at UPV [24] precisely covers the whole UWB frequency band and it is the most accurate so far in the literature.

A magnetic sensor is attached to the in-body and on-body antennas so that the tracker (Fig. 2, element 4ab) can precisely evaluate the distance between antennas as well as their respective coordinates according to the magnetic transmitter reference system (Fig. 3).

Measurements were performed by moving the in-body antenna, placed inside the muscle layer, in steps of 1 cm along the *x*-, *y*-, and *z*-axes with a grid size of (Nx = 12, Ny = 11, and Nz = 2), as depicted in Fig. 3. Five on-body antenna positions, with a separation of 2 cm, along y as well as along the *z*-axis, were considered on the outer edge of the fat layer (Fig. 3).

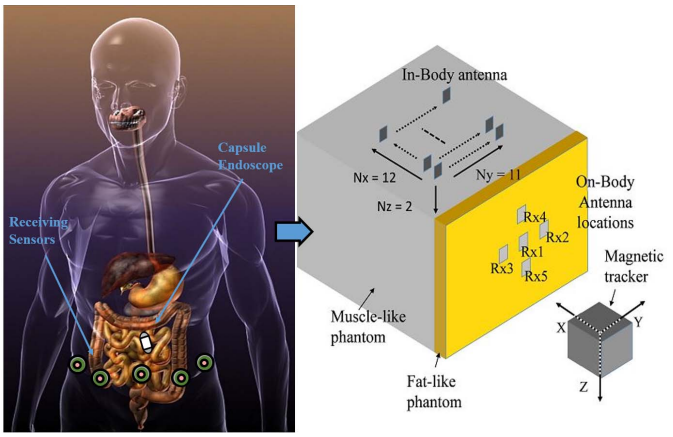

Fig. 3. WCE procedure versus experimental measured grid.

In order to improve the signal-to-noise ratio (SNR) for each in-body antenna position on the grid and each on-body receiver, five snapshots of the channel (S_{21}) were taken, considering 3201 resolution points in frequency. Only values above the noise level (–90 dB) were taken into account. For each snapshot, the tracker calculated the distance between antennas, as well as in-body and on-body (x, y, and z) antenna coordinates, 100 times.

By averaging the collected data, S_{21}, antenna separation and antenna coordinates were evaluated.

B. In Vivo Measurements

In vivo measurements were conducted in a living porcine model, at the animal laboratory of the Hospital Universitari i Politècnic la Fe in Valencia, Spain, after approval by the Ethical Committee of Investigation of the hospital, under the protocol WIBEC 2015/0463. A brief description of the experiment is given in this section, in order to highlight the main aspects. Further and more detailed information can be found in [30].

Same equipment (VNA and magnetic tracker) described in Section III-A for the phantom measurements campaign was used. As the main scenario of interest for WCE applications is the GI tract, the in-body antenna was placed, through laparoscopy, in three different positions inside the abdomen of the porcine model, in order to be surrounded by either small bowel or colon or both. For each in-body location, the on-body antenna was placed inside the abdomen of a porcine model, in direct contact with the skin [Fig. 4(a)], in 13 different locations, as depicted in Fig. 4(b).

Measurements were taken in the 3–6 GHz UWB frequency band, considering 1601 resolution points in frequency. Through the VNA, for each pair of in-body to on-body positions, five snapshots of the channel (S_{21}) were taken. Again, only values above the noise level (-90 dB) were taken into account.

As for the phantom measurements, antenna separation distance and antenna coordinates were evaluated 100 times per snapshot by the magnetic tracker. Finally, by averaging the collected measurements, S_{21}, the antenna separation distance and antenna coordinates were evaluated.

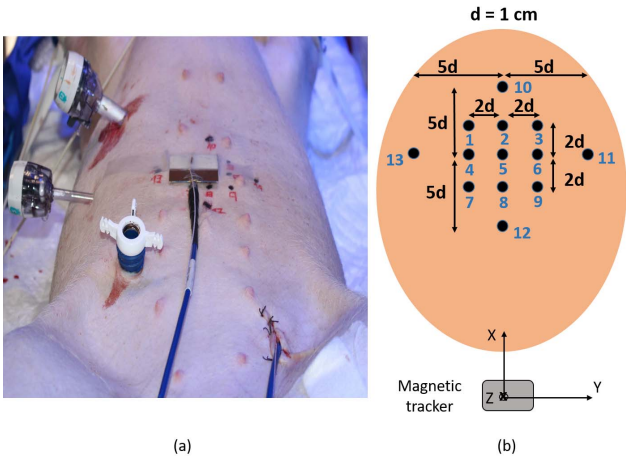

Fig. 4. (a) *In vivo* measurements for one on-body position and (b) measured grid for each in-body position (top view).

IV. RSS-Based Ranging and Localization Algorithms

For both the measurement campaigns, data from 3.1 to 5.1 GHz are considered because for antenna distances larger than 8–9 cm, measurements beyond 5.1 GHz are below the noise level [26].

From the measured S_{21}, the PL is evaluated for each in-body to on-body antenna position as follows:

$$PL_{meas}(dB) = -10\log_{10}(mean(|H(f)|^2)). \tag{1}$$

where $H(f)$ is the frequency-domain transfer function in N resolution points computed as $H(f) = |S_{21}|e^{-j\phi S_{21}}$, being $|S_{21}|$ and ϕ_{S21} the module and phase in radians of S_{21}, respectively.

For both the measurement campaigns, PL values within a distance of 8 cm between in-body and on-body antenna centers are selected due to the noise level, as pointed out at the beginning of this section.

Selected PL values are then fitted by a log-distance approximation model as follows:

$$PL(dB) = PL_{0,d_{ref}}(dB) + 10n\log_{10}\left(\frac{d}{d_{ref}}\right) \tag{2}$$

where d is the distance between antenna centers, d_{ref} is the reference distance at 1 cm, $PL_{0,d_{ref}}$ is the PL at d_{ref}, and n is the PL exponent.

From measurements, the performance of RSS-based positioning is evaluated and compared under two different assumptions.

1) Assuming an ideal receiver capable of detecting all the multipath components of the channel impulse response (ideal case) through (1), the PL can be precisely estimated as

$$PL_{est}(dB) = PL_{meas}(dB). \tag{3}$$

2) Considering a real case scenario, where the receiver receives for a given period of time being able to detect only a few multipath components with power below a certain level from the strongest path, the PL can be computed as follows:

$$PL_{est}(dB) = -10\log_{10} sum(|h(\tau)|^2_{sel}) \tag{4}$$

where $|h(\tau)|_{sel} = |\text{ifft}(H(f))|_{sel}$ are the selected multipath components of the channel impulse response.

From the model proposed in (2), an estimation of d can be obtained as follows:

$$d_{est} = 10^{\frac{PL_{est}-PL_{0,d_{ref}}}{10n}} \cdot d_{ref} \tag{5}$$

where PL_{est} is the PL evaluated using (3) or (4) if assuming ideal or nonideal channel estimation, respectively.

A. 2-D Phantom-Based Postprocessing

For the multilayer phantom measurements, only two coordinates of the in-body antenna (y and z) can be evaluated as all receivers share the same x-coordinate (Fig. 3). In order to estimate the in-body antenna coordinates, the adaptive linearized method described in [31] is adapted in [32] and implemented for the 2-D case. Three receivers are required to find the unique solution of the linearized system of two equations in two unknowns. Not more than three receivers are used to evaluate the 2-D localization performance. Due to the number of receivers (only five) and their configuration (Fig. 3), using four or all five receivers and applying minimization error techniques does not improve the estimation accuracy of the in-body antenna coordinates.

B. 3-D In Vivo Postprocessing

Regarding the *in vivo* measurements, one of the in-body positions was discarded because the antenna separation distances were above 8 cm for all on-body receiver positions.

A general PL model is calculated through (2) considering all the on-body antenna locations [Fig. 4(b)] and the two in-body positions under study. For 3-D localization, if applying the adaptive linearized method, four receivers are required to directly solve the system of three equations in three unknowns. Since *in vivo* measurements are not as many as those performed in the laboratory with phantom and due to animal's respiration, PL values present a high standard deviation with respect to the evaluated fit model [30]. Therefore, for 3-D localization, the method described in [33] is used. More than four receivers are selected for positioning. The first estimation of the in-body antenna coordinates is obtained through the linear least square method. Then, the nonlinear least square (NLLS) approach is applied. The sum of the square errors is minimized through the Levenberg–Marquardt algorithm [34]. Further details regarding the selection criteria of the receivers and the performance metrics used to evaluate the results are given in Section V.

V. Results

A. Performance Metrics

In order to assess the achieved localization accuracy, the localization error, *LE*, for the 3-D case and its relative

error can be defined as

$$LE = \sqrt{(x_{IB}-x_{IB\_est})^2+(y_{IB}-y_{IB\_est})^2+(z_{IB}-z_{IB\_est})^2} \tag{6}$$

$$RelLE = \frac{LE}{\sqrt{x_{IB}^2+y_{IB}^2+z_{IB}^2}} \tag{7}$$

where (x_{IB}, y_{IB}, z_{IB}) and $(x_{IB\_est}, y_{IB\_est}, z_{IB\_est})$ are the real and estimated coordinates of the in-body antenna, respectively.

For the 2-D case, (6) and (7) are calculated omitting the x-coordinate since for the specific receiver configuration (Fig. 3), it cannot be estimated.

Moreover, the relative errors on the estimation of the in-body antenna coordinates can be evaluated individually as follows:

$$RelErr_{x_{IB}} = \frac{|x_{IB\_est}-x_{IB}|}{|x_{IB}|} \tag{8}$$

$$RelErr_{y_{IB}} = \frac{|y_{IB\_est}-y_{IB}|}{|y_{IB}|} \tag{9}$$

$$RelErr_{z_{IB}} = \frac{|z_{IB\_est}-z_{IB}|}{|z_{IB}|}. \tag{10}$$

B. 2-D Localization Results

As detailed in Section IV, for the multilayer phantom-based measurements, PL values related to antenna distances up to 8 cm are fitted through (2), being $d_0 = 1$ cm, $PL_{0,dref} = -24.43$ dB, and $n = 9.69$.

In order to estimate the (y_{IB}, z_{IB}) coordinates of the in-body antenna, different combinations of three receivers (one taken as reference) were considered to directly solve the linearized system in [31] with two equations. Fig. 5(a) depicts the cumulative distribution function (CDF) of the relative localization error, computed as in (7), for three different combinations of three receivers. In Fig. 5(b), the true locations of the in-body antenna (given by the magnetic tracker) are represented versus the estimated ones for the same combinations of receivers. Results show how the receivers selected for localization impact the accuracy of the results. Particularly, the combination of receivers 2, 4, and 3, taken as reference, leads to lower relative error values compared to the other combinations, as it is experiencing, on average, the highest level of received power [35], [36]. Similar results were obtained for the same combinations of receivers in a narrower frequency band (3.1–4.1 GHz) [32].

Considering the combination of receivers leading to the best performance, i.e., receivers 2, 4, and 3 as reference (Fig. 5), localization accuracy was evaluated and compared in the case of ideal and nonideal channel estimation assumptions, detailed in Section IV. As already mentioned, in the case of ideal channel (case 1), the PL is computed as in (1). In the case of nonideal channel (case 2), the PL is evaluated through (4), by selecting all the multipath components whose power is above or equal to the maximum of the power delay profile minus a certain threshold, specifically 5, 10, and 20 dB, respectively.

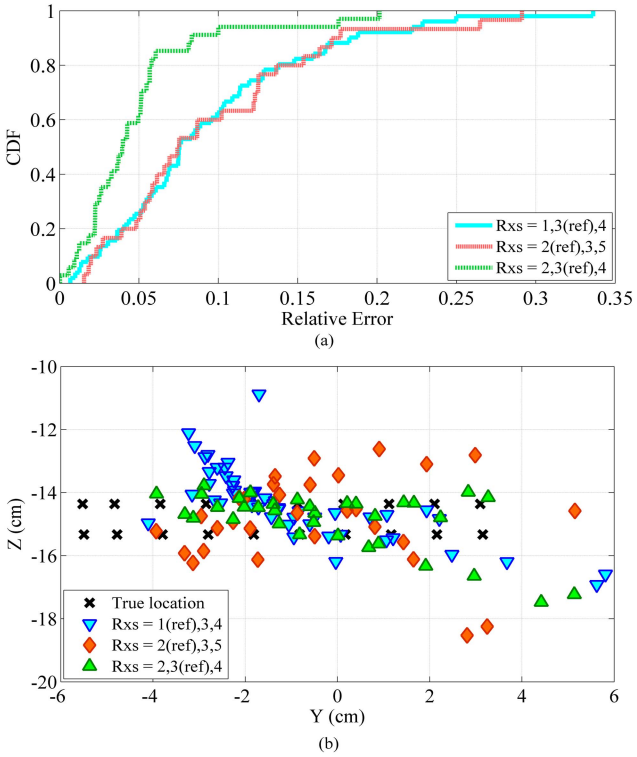

Fig. 5. (a) CDF of the relative localization error. (b) True location versus estimated location of the in-body antenna.

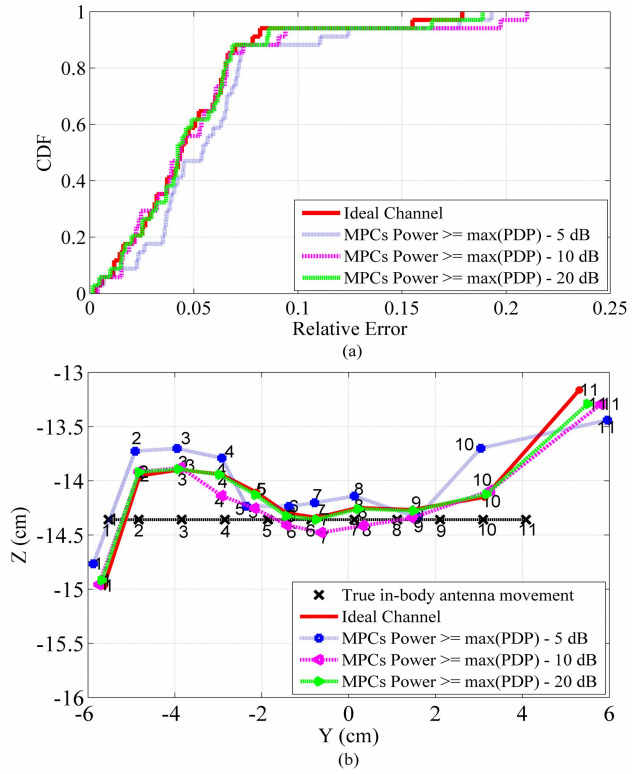

Fig. 6. (a) Relative localization error and (b) example of tracking the in-body antenna moving along the y-axis, for $x = 1$ and $z = 2$, for ideal and nonideal channels.

Fig. 6(a) shows that considering the components with power below 10 dB/20 dB from the maximum (magenta and green curve), almost same performance as for the ideal channel

case is obtained, while slightly worse performance is observed when considering the components below 5 dB (blue curve). This is also observed in Fig. 6(b), where using the same combination of receivers, an example of tracking considering the in-body antenna moving in steps of 1 cm along the y-axis, for $x = 1$ and $z = 2$, is presented. It is important to mention that, for this track, the distance between the in-body antenna and some on-body receivers is sometimes higher than 8 cm. Thus, for such points, the PL model used for ranging estimation does not include such distances, leading to some inaccuracies. In fact, it is worth observing in Fig. 6(b) that, for all the considered cases, the estimation error is higher for the outer points of movement of the in-body antenna, i.e., 1–4, 10, and 11. For these positions, the distance between the in-body antenna and receivers 2 and 3 is outside the region of validity of the evaluated PL model. This means more inaccuracy in the ranging distance calculation in (5) and, consequently, more uncertainty in the estimation of the in-body antenna coordinates (y_{IB}, z_{IB}).

Regarding the localization performance, considering the ideal channel estimation (case 1), an average relative localization error of 4.7% corresponding to an LE = 0.72 cm is achieved. For the nonideal channel estimation (case 2), considering components with power below 5 dB from the maximum, an average relative error of 5.7% (LE = 0.86 cm) is obtained. This means that, in a realistic scenario (nonideal channel estimation), the inability of the receiver to perfectly characterize the channel affects the positioning accuracy leading to an increase of 1% in the localization error, which is under study.

C. 3-D Localization Results

For the *in vivo* measurements, as detailed in Section IV, PL values related to antenna distances below or equal to 8 cm are fitted through (2), as for the 2-D case, resulting in $d_0 = 1$ cm, $PL_{0,dref} = 21.84$ dB, and $n = 5.44$. In this case, the dispersion of the PL values with respect to the fitting model is higher [root mean square error (RMSE) $\sim$ 28] [30]. This is due to the fact that measurements were conducted in a realistic and different scenario with respect to the laboratory environment. Moreover, much less measurement points with respect to the laboratory measurement campaign are available to derive a PL model, as mentioned in Section IV-B.

In order to compare the goodness of the localization method, in-body antenna coordinates were first estimated as for the 2-D case, i.e., by solving the linearized system in [31] using four receivers (3-D case). Performance in terms of the relative localization error, computed as in (7), is presented in Table I. Labels Tx1 and Tx2 indicate the error values related to the first and second in-body positions under study, respectively. Results show that this localization method, unlike for the 2-D case, is not suitable in this realistic scenario, leading to high inaccuracy, especially for in-body position Tx2. In order to improve the performance, as mentioned in Section IV-B, the NLLS method was applied to minimize possible inaccuracy in the ranging distance estimation through the derived PL model. Results obtained by applying such a method for different number of receivers are presented in Table I. For each case, receivers experiencing the highest relative received power were selected.

TABLE I
LOCALIZATION ERRORS FOR DIFFERENT APPROACHES

	Rel_{LE} (%)	
Method	Tx1	Tx2
Linearized System	38.5	2848
NLLS (7 Rxs)	1.81	1.41
NLLS (10 Rxs)	1.48	1.40
NLLS (13 Rxs)	1.21	2.82

TABLE II
LOCALIZATION ERRORS USING DIFFERENT PL MODELS

	Rel_{LE} (%)	
PL Model	Tx1	Tx2
General *In Vivo*	1.52	1.66
Phantom-based	4.48	6.13

Results in Table I show that implementing the NLLS method significantly improves the estimation accuracy, especially for the second in-body position whose relative error drops up to 1.5%, by using 7/10 receivers. However, by increasing the number of receivers from 7 to 10 and from 7 to 13, the relative localization error slightly decreases for in-body position Tx1 but not for position Tx2. In fact, passing from 10 to 13 receivers means, for in-body position Tx1, that there is one receiver outside the region of validity of the PL model ($\geq$8 cm), and for position Tx2, there are three of them. This clearly affects the ranging accuracy and adds uncertainty when applying the minimization error algorithm. As for both in-body positions, increasing the number of receivers up to 10 leads to fairly good performance; results presented in the remainder of this section were obtained applying the Levenberg–Marquardt algorithm by selecting those ten receivers experiencing the highest power.

In order to compare the goodness of the obtained PL model for the 2-D case, 3-D localization performance was evaluated by using the phantom PL model given in Section V-B. Table II shows the comparison of the relative localization error obtained using the general PL model derived from the *in vivo* measurements with the one derived from the multilayer phantom-based measurements. Using the phantom model leads to an increment of 3%–4% in the localization error.

As explained at the beginning of this section, due to the differences between the two PL models, better results, as expected, were obtained by using the fitting model related to the specific scenario (*in vivo*).

As for the 2-D case, performance considering the ideal and nonideal channels was evaluated. Tables III and IV report, for in-body positions Tx1 and Tx2, respectively, the localization error LE and its relative error Rel_{LE} as well as the relative and absolute errors in the estimation of x_{IB}, y_{IB}, and z_{IB} for ideal and nonideal channel cases, using the general *in vivo* PL model.

Results, considering ideal and nonideal channels, show that the lowest localization errors are obtained in the estimation of x_{IB} for both in-body positions. As reported in Table III,

TABLE III
LOCALIZATION ERRORS FOR IN-BODY POSITION TX1

	Ideal	-10 dB	-5 dB
Rel_{LE} (%)	1.48	1.27	1.11
LE (cm)	0.97	0.83	0.72
$RelErr_{x_{IB}}$ (%)	1.03	0.93	0.81
$AbsErr_{x_{IB}}$ (cm)	0.66	0.60	0.52
$RelErr_{y_{IB}}$ (%)	5.93	4.85	2.87
$AbsErr_{y_{IB}}$ (cm)	0.28	0.23	0.14
$RelErr_{z_{IB}}$ (%)	6.40	5.19	4.77
$AbsErr_{z_{IB}}$ (cm)	0.65	0.52	0.48

TABLE IV
LOCALIZATION ERRORS FOR IN-BODY POSITION TX2

	Ideal	-10 dB	-5 dB
Rel_{LE} (%)	1.40	1.71	1.86
LE (cm)	0.91	1.12	1.21
$RelErr_{x_{IB}}$ (%)	0.55	0.78	0.41
$AbsErr_{x_{IB}}$ (cm)	0.35	0.50	0.26
$RelErr_{y_{IB}}$ (%)	6.44	8.65	5.53
$AbsErr_{y_{IB}}$ (cm)	0.21	0.29	0.18
$RelErr_{z_{IB}}$ (%)	8.34	9.81	11.99
$AbsErr_{z_{IB}}$ (cm)	0.82	0.96	1.17

for in-body position Tx1, error values calculated considering the ideal channel are slightly higher than those obtained for the nonideal channel case. For in-body position Tx2, same behavior is observed in the estimation of x_{IB} and y_{IB}, as given in Table IV. Although the difference between error values in both the cases is not critical, this closely depends on the evaluated PL model, as described in Section IV-B. As pointed out in the same section, few *in vivo* measurement points are available to derive a model. In fact, as detailed in [30], measured PL values present a higher standard deviation with respect to the calculated fitting model, compared to the 2-D case. Moreover, the pig's respiration might also have been affecting the relative received power and thus the accuracy of the localization.

VI. DISCUSSION AND FUTURE WORK

Summarizing the results, it was found that, for the 2-D case, the combination of three receivers experiencing the highest power leads to the best performance in terms of relative localization error. This is in line with the way the current WCE localization algorithms work [36], [37]. Considering the ideal channel estimation, an average relative localization error of 4.7% (0.72 cm) has been obtained. For the nonideal channel estimation case, the accuracy slightly decreases, as expected, resulting in a relative localization error on average of 5.7% (0.86 cm).

For 3-D localization, the best performance was achieved by selecting those ten receivers experiencing the highest received power. In the case of ideal channel estimation, considering both in-body locations under study, an average relative localization error of 1.4% (0.94 cm) has been obtained. For the nonideal channel estimation case, the localization error is slightly lower, with respect to the ideal case, due to the derived PL model.

It is important to mention that, for both laboratory and *in vivo* measurements, the orientation of the in-body and on-body antennas was kept the same, in order to better investigate the effect of the propagation channel on the localization performance. In real applications, this condition is not satisfied at all and the unknown orientation of the capsule inside the GI tract affects the localization accuracy. As part of the future work, further experimental measurements could be performed to take into account the misorientation between the antennas. As a matter of fact, the directionality (or null) in the radiation pattern of the transmitting antenna could be exploited to estimate its orientation through several on-body receivers, as presented in [38].

In addition, a possible solution to overcome signal losses, due to orientation changes of the in-body antenna, could be the use of circularly polarized in-body antennas that are less vulnerable to polarization mismatches and multipath distortion.

Results presented in this paper show the importance of the PL model for the localization using the RSS. Although the methodology used is valid for any separating distance between the in-body and on-body antennas, the derived PL models are not valid for antennas with a distance above 8 cm due to our particular measurement setup. More extensive measurement campaigns are being arranged in order to derive a more accurate and general PL model as well as, in case of *in vivo* experiment, further studies on the impact of animal's respiration on the received power are being conducted.

Finally, the combination of the RSS-based approach with other localization techniques (image-based, for example) is explored in order to improve the positioning accuracy.

VII. CONCLUSION

In this paper, the performance of the RSS-based localization technique, for in-body to on-body communications in the 3.1–5.1 GHz UWB frequency band, has been investigated through experimental laboratory measurements and *in vivo* experiment. 2-D localization is performed using experimental measurements conducted through a customized multilayer phantom-based testbed. In this case, an adaptive linearized method, considering different combinations of three receivers, is sufficient to estimate the in-body antenna coordinates. 3-D localization is performed using data collected during a recently conducted *in vivo* experiment in a living pig. In this more realistic case, due to the high dispersion of the PL values with respect to the fitting model, least square and NLLS methods have been implemented for the estimation of the in-body antenna coordinates. For both 2-D and 3-D cases, performance obtained under the assumption of ideal and nonideal channel estimations has been analyzed.

Results presented in this paper constitute a first step in the testing of RF-based localization techniques in more realistic environments compared to software simulations platforms.

REFERENCES

[1] G. Ciuti, A. Menciassi, and P. Dario, "Capsule endoscopy: From current achievements to open challenges," *IEEE Rev. Biomed. Eng.*, vol. 4, pp. 59–72, Oct. 2011.

[2] M. F. Hale, R. Sidhu, and M. E. McAlindon, "Capsule endoscopy: Current practice and future directions," *World J. Gastroenterol.*, vol. 20, no. 24, pp. 7752–7759, 2014.

[3] *Medtronic*. [Online]. Available: https://www.medtronic.com/covidien/en-us/products/capsule-endoscopy/pillcam-sb-3-system.html

[4] D. M. Pham and S. M. Aziz, "A real-time localization system for an endoscopic capsule using magnetic sensors," *Sensors*, vol. 14, no. 11, pp. 20910–20929, Sep. 2014.

[5] K. Pahlavan *et al.*, "RF localization for wireless video capsule endoscopy," *Int. J. Wireless Inf. Netw.*, vol. 19, no. 4, pp. 326–340, Dec. 2012.

[6] M. Pourhomayoun, M. Fowler, and Z. Jin, "A novel method for medical implant in-body localization," in *Proc. Annu. Int. Conf. IEEE Eng. Med. Biol. Soc. (EMBS)*, Aug./Sep. 2012, pp. 5757–5760.

[7] C. Hu, M. Q. Meng, and M. Mandal, "Efficient magnetic localization and orientation technique for capsule endoscopy," in *Proc. IEEE/RSJ Int. Conf. Intell. Robots Syst.*, Aug. 2005, pp. 3365–3370.

[8] R. Kuth, J. Reinschke, and R. Rockelein, "Method for determining the position and orientation of an endoscopy capsule guided through an examination object by using a navigating magnetic field generated by means of a navigation device," U.S. Patent 20070038063 A1, Feb. 15, 2007.

[9] G. Bao, L. Mi, and K. Pahlavan, "A video aided RF localization technique for the wireless capsule endoscope (WCE) inside small intestine," in *Proc. 8th Int. Conf. Body Area Netw.*, Feb. 2016, pp. 55–61.

[10] J. Lee, J. Oh, S. K. Shah, X. Yuan, and S. J. Tang, "Automatic classification of digestive organs in wireless capsule endoscopy videos," in *Proc. ACM Symp. Appl. Comput.*, 2007, pp. 1041–1045.

[11] G. Bao and K. Pahlavai, "Motion estimation of the endoscopy capsule using region-based Kernel SVM classifier," in *Proc. IEEE Int. Conf. Electro-Inf. Technol.*, May 2013, pp. 1–5.

[12] U. I. Khan, K. Pahlavan, and S. Makarov, "Comparison of TOA and RSS based techniques for RF localization inside human tissue," in *Proc. Annu. Int. Conf. IEEE Eng. Med. Biol. Soc. (EMBS)*, Aug./Sep. 2011, pp. 5602–5607.

[13] A. Nafchi, S. T. Goh, and S. R. Zekavat, "Circular arrays and inertial measurement unit for DOA/TOA/TDOA-based endoscopy capsule localization: Performance and complexity investigation," *IEEE Sensors J.*, vol. 14, no. 11, pp. 3791–3799, Nov. 2014.

[14] Y. Geng and K. Pahlavan, "On the accuracy of RF and image processing based hybrid localization for wireless capsule endoscopy," in *Proc. IEEE Wireless Commun. Netw. Conf. (WCNC)*, Mar. 2015, pp. 452–457.

[15] G. Bao, "On simultaneous localization and mapping inside the human body (body-slam)," Ph.D. dissertation, Dept. ECE, WPI, Worcester, MA, USA, 2014.

[16] A. S. Bjørnevik, "Localization and tracking of intestinal paths for wireless capsule endoscopy," M.S. thesis, Dept. DET, Norwegian Univ. Sci. Technol., Trondheim, Norway, 2015.

[17] M. R. Yuce, H. C. Keong, and M. S. Chae, "Wideband communication for implantable and wearable systems," *IEEE Trans. Microw. Theory Techn.*, vol. 57, no. 10, pp. 2597–2604, Oct. 2009.

[18] J. Wang and Q. Wang, *Body Area Communications: Channel Modeling, Communication Systems, and EMC*. Hoboken, NJ, USA: Wiley, 2013.

[19] H. Mateen, R. Basar, A. U. Ahmed, S. Member, and M. Y. Ahmad, "Localization of wireless capsule endoscope: A systematic review," *IEEE Sensors J.*, vol. 17, no. 5, pp. 1197–1206, Mar. 2017.

[20] B. Moussakhani, J. T. Flam, S. Stoa, I. Balasingham, and T. Ramstad, "On localisation accuracy inside the human abdomen region," *IET Wireless Sensor Syst.*, vol. 2, no. 1, pp. 9–15, Mar. 2012.

[21] M. Kanaan and M. Suveren, "In-body ranging with ultra-wideband signals: Techniques and modeling of the ranging error," *Wirel. Commun. Mobile Comput.*, vol. 2017, Jan. 2017, Art. no. 4313748.

[22] Y. Ye, "Bounds on RF cooperative localization for video capsule endoscopy," Ph.D. dissertation, Dept. ECE, WPI, Worcester, MA, USA, 2013.

[23] S. Castello-Palacios, C. Garcia-Pardo, A. Fornes-Leal, N. Cardona, and A. Vallês-lluch, "Tailor-made tissue phantoms based on acetonitrile solutions for microwave applications up to 18 GHz," *IEEE Trans. Microw. Theory Techn.*, vol. 64, no. 11, pp. 3987–3994, Nov. 2016.

[24] N. Cardona, S. Castello-Palacios, A. Fornes-Leal, C. Garcia-Pardo, and A. Vallês-lluch, "Synthetic model of biological tissues for evaluating the wireless transmission of electromagnetic waves," WO Patent 2017109252 A1, Jan. 30, 2017.

[25] S. Castelló-palacios, C. Garcia-pardo, A. Fornes-leal, N. Cardona, and A. Vallês-lluch, "Full-spectrum phantoms for cm-wave and medical wireless communications," in *Proc. 12th Eur. Conf. Antennas Propag.*, Apr. 2018, pp. 1-3.

[26] S. Perez-Simbor, M. Barbi, C. Garcia-Pardo, S. Castelló-Palacios, and N. Cardona, "Initial UWB in-body channel characterization using a novel multilayer phantom measurement setup," in *Proc. IEEE Wireless Commun. Netw. Conf. (WCNCW)*, Apr. 2018, pp. 384–389.

[27] (Feb. 2015). *Medtronic RAPID Software User Manual*. [Online]. Available: https://www.medtronic.com/content/dam/covidien/library/us/en/product/diagnostic-testing/rapid-v83-user-manual.pdf

[28] C. Andreu, C. Garcia-Pardo, A. Fornes-Leal, M. Cabedo-Fabrés, and N. Cardona, "UWB in-body channel performance by using a direct antenna designing procedure," in *Proc. 11th Eur. Conf. Antennas Propag. (EUCAP)*, Mar. 2017, pp. 278–282.

[29] C. Tarin, P. Marti, L. Traver, N. Cardona, J. A. Diaz, and E. Antonino, "UWB channel measurements for hand-portable devices: A comparative study," in *Proc. IEEE 18th Int. Symp. Pers., Indoor Mobile Radio Commun. (PIMRC)*, Sep. 2007, pp. 1–5.

[30] S. Perez-Simbor, C. Andreu, C. Garcia-Pardo, M. Frasson, and N. Cardona, "UWB path loss models for ingestible devices," *IEEE Trans. Antennas Propag.*, to be published.

[31] K. Arshak and F. Adepoju, "Adaptive linearized methods for tracking a moving telemetry capsule," in *Proc. IEEE Int. Symp. Ind. Electron.*, Jun. 2007, pp. 2703–2708.

[32] M. Barbi, S. Perez-Simbor, C. Garcia-Pardo, C. Andreu, and N. Cardona, "Localization for capsule endoscopy at UWB frequencies using an experimental multilayer phantom," in *Proc. IEEE Wireless Commun. Netw. Conf. Workshops (WCNCW)*, Apr. 2018, pp. 390–395.

[33] W. Murphy and W. Hereman, "Determination of a position in three dimensions using trilateration and approximate distances," Ph.D. dissertation, Dept. Math. Comput. Sci., Colorado School Mines, Golden, CO, USA, vol. 95, vol. 7, 1995, p. 19.

[34] C. L. Lawson and R. J. Hanson, *Solving Least Squares Problems*. Philadelphia, PA, USA: SIAM, 1995.

[35] I. Umay, B. Fidan, and B. Barshan, "Localization and tracking of implantable biomedical sensors," *Sensors*, vol. 17, no. 3, p. 583, 2017.

[36] T. D. Than, G. Alici, H. Zhou, and W. Li, "A review of localization systems for robotic endoscopic capsules," *IEEE Trans. Biomed. Eng.*, vol. 59, no. 9, pp. 2387–2399, Sep. 2012.

[37] M. R. Basar, F. Malek, K. M. Juni, M. S. Idris, and M. I. M. Saleh, "Ingestible wireless capsule technology: A review of development and future indication," *Int. J. Antennas Propag.*, vol. 2012, Dec. 2012, Art. no. 807165.

[38] K. Krhac, K. Sayrafian, M. Alasti, K. Y. Yazdandoost, and D. Simunic, "A study of capsule endoscopy orientation estimation using received signal strength," in *Proc. PIMRC*, Sep. 2018, pp. 345–349.

Martina Barbi was born in Reggio Emilia, Italy, in 1985. She received the M.S. degree in telecommunication engineering from the University of Bologna, Bologna, Italy, in 2012. She is currently pursuing the Ph.D. degree in technologies for health and well-being with the Institute of Telecommunications and Multimedia Applications (iTEAM), Universitat Politècnica de València (UPV), Valencia, Spain.

From 2012 to 2016, she was with the National Institute of Standards and Technology (NIST), Gaithersburg, MD, USA, as a Contract Researcher in the development of interference mitigation techniques for body area networks (BANs). She is currently a Contract Researcher with WiBEC ITN (Wireless In Body Environment–Marie Curie Skłodowska Actions), iTEAM, UPV. Since 2016, she has been a Researcher with iTEAM. She has authored or coauthored three journal and five conference papers. Her current research interests include wireless medical communications, RF-based localization, tracking for capsule endoscopy at UWB frequencies, and the development and testing of localization techniques for capsule endoscopy applications at UWB frequencies.

Concepcion Garcia-Pardo received the degree in telecommunication engineering, the M.Sc. degree in information technologies and communications, and the Ph.D. degree (*cum laude*), with European mention and qualification, from the Universidad Politécnica de Cartagena, Cartagena, Spain, in 2007, 2008, and 2012, respectively, and the Ph.D. degree in microwaves and microtechnologies, with qualification Très Honorable, from Lille 1 University, Villeneuve-d'Ascq, France. Her Ph.D. dissertation received the special prize from the Universidad Politécnica de Cartagena in 2013.

In 2012, she joined the Institute of Telecommunications and Multimedia Applications (iTEAM), Universitat Politècnica de Valencia, Valencia, Spain, where she was a Senior Researcher. She has authored more than 40 publications of journal and conference papers related to wireless communications. She has also participated in several national and international project related to wireless communications and wireless medical devices. She is also part of the management committee of COST Action CA 15104-IRACON. Her current research interests include wireless medical devices and wireless communications for body area networks.

Dr. Garcia-Pardo regularly serves as a reviewer for the main journals related to electromagnetism and propagation.

Andrea Nevárez was born in Quito, Ecuador. She received the Ph.D. degree in medicine from the Pontificia Universidad Católica of Ecuador, Quito, in 2003. She is currently pursuing the Ph.D. degree with the Medical Department, Universitat de València Spain. She is currently pursuing the Ph.D. degree with the University and Polytechnic Hospital La Fe, Valencia. She received the Fellowship in gastroenterology from the University and Polytechnic Hospital La Fe, Valencia, in 2010.

In 2010, she attended for two months as an Exchange Fellow with the MD Anderson Cancer Center, Houston, TX, USA. From 2010 to 2016, she was a Digestive Endoscopist in her home country. She is also an Early Stage Researcher for WiBEC ITN (Wireless In Body Environment–Marie Curie Skłodowska Actions). She has coauthored four papers published in indexed journals and also has presented oral communications in international meetings. Her current research interests include the development of medical devices and computer-aided diagnosis systems applied to the digestive system.

Ms. Nevárez is a member of the Spanish Digestive Endoscopic Society (SEED) and is a part of the study group in capsule endoscopy and enteroscopy.

Vicente Pons Beltrán was born in Valencia, Spain, in 1965. He received the Ph.D. degree in medicine from the University Miguel Hernández de Elche, Elche, Spain, in 2001. He received the Gastroenterology Fellowship in 1994.

He is currently the Head of the Digestive Endoscopy Unit, University and Polytechnic Hospital La Fe, Valencia. Almost from the beginning of his professional career, he has developed his work linked to gastrointestinal endoscopy, primarily in the area of the biliopancreatic tree and small bowel endoscopy. He has conducted research projects on the field of endoscopic capsule and on the development of an enteroscopy prototype. He has authored several international publications related to capsule endoscopy. He worked for more than 10 years together with researchers from the Department of Applied Physics, Energy Engineering Institute, Technical College Engineering Design, Polytechnic University of Valencia, and has led several research projects in biomedical research (Endoworm Project).

Dr. Pons Beltrán is regularly invited as a speaker at symposiums and conferences in gastrointestinal endoscopy. He is the President of the Foundation of the National Spanish Digestive Endoscopy Society.

Narcís Cardona (M'91) was born in Barcelona, Spain. He received the M.S. degree in communications engineering from ETSI Telecommunications, Universitat Politècnica de Catalunya, Barcelona, in 1990, and the Ph.D. degree in telecommunications from the Universitat Politècnica de València, Valencia, Spain, in 1995.

Since 1990, he has been with the Communications Department, Universitat Politècnica de València, where he became a Full Professor in 2006. He is currently the Head of the Mobile Communications Group and the Director of the Research Institute of Telecommunications and Multimedia Applications (iTEAM), Universitat Politècnica de València, a research institute with around 150 researchers, including an Assistant Professors and a Research Fellows. He has authored several research books and more than 200 publications in the most relevant international journal and conferences of the communications field. He holds ten patents. His current research interests include mobile channel characterization, broadcast cellular hybrid networks, and body area networks.

Dr. Cardona has been the Vice Chairman of COST273, the Chair of the WG3 in COST2100, the General Chair of COST IC1004, and the Vice Chairman of COST IC15104 IRACON since 2016. He is a member of the Steering Committee of METIS (7FP), METIS-II (H2020 5GPPP), and WIBEC (H2020 ITN) from 2016 to 2019. He is a Coordinator of WaveComBE (ITN) from 2017 to 2021. He has also organized several international conferences, such as ISWCS 2006, IEEE PIMRC 2016, and EuCNC 2019.